UNIVERSITÀ
DI TRENTO

DIPARTIMENTO DI FISICA

LAUREA IN FISICA

Development of an electronic chaotic circuit on the “RemoteLab” platform

Supervisore:
Leonardo Ricci

Laureando:
Simone Girardi

ANNO ACCADEMICO: 2021/2022

DATA ESAME FINALE: 22/09/2022

1 Introduction

Throughout this paper we will verify the chaotic behaviour of the Chua's Circuit using the sound card of a computer as an oscilloscope and a function generator thanks to the "RemoteLab" software package. Before starting with the circuit analysis it's important to understand what the Chaotic behaviour is.

In contrast with the popular belief Chaos isn't something random generated, instead it's governed by known deterministic equations.

A system in order to be chaotic needs to meet three criteria: Topological transitivity, Density of periodic orbits and Sensibility to initial conditions.

The first two criteria are more mathematical concepts. The system has to evolve in such a way that two open sets in phase space will eventually overlap, this propriety is called Topology transitivity. Density of periodic orbit on the other hand requires that every point in phase space is arbitrarily close to a periodic orbit. From these two characteristics it can be deducted that the trajectories can transit in all of phase space but is empirically verified that the chaotic motion is confined in a restricted area, this is caused by the presence of attractors. An attractor is a region of phase space to which the surrounding trajectories are attracted. It can be a point, a curve or, more generally, a manifold. There are two principal types of attractors: Strange and Nonstrange. An attractor is strange if the attracting set presents a fractal nature. This is not to be confused with a consequence of a chaotic behaviour although a chaotic system always features a strange attractor [3].

The latter criteria is the most meaningful one. A chaotic system in fact is very sensitive to the initial conditions, meaning that even a minor difference of at least one of the initial conditions will significantly change the outcome. This characteristic is popularly known as "Butterfly Effect" due to Edward Norton Lorentz that chose as a title for one of his talk: "Does the flap of a butterfly's wings in Brazil set off a tornado in Texas?".

E. N. Lorentz understood that a chaotic system follows the Butterfly Effect when he was making computations for weather forecasting. He used a complicated set of equations with 12 parameters and made a Royal McBee LGP-30 computer calculate the outcome for various iterations. When he decided to repeat the calculations he inserted a line of numbers that the computer had printed out earlier. The outcome was at first coherent but then became substantially different from the previous one. The justification is "simple": when he inserted the numbers for the recalculation he changed the initial condition by omitting the last significant digits. Being the system chaotic this little mistake made clear the sensibility to the initial conditions of the weather differential equations.

A mathematical way to describe this sensibility from the initial condition does exist, it's called "Lyapunov exponent" and is used primarily for identifying chaos [8].

The Lyapunov exponent λ is defined using the difference $\delta(t)$ between the trajectories in phase space as follow:

$$|\delta(t)| = \delta_0 e^{\lambda t} \qquad where \qquad \delta_0 = \ Initial\ separation \tag{1.0.1}$$

The Lyapunov exponent can be either positive or negative. If $\lambda > 0$ the system is called Chaotic because two trajectories will diverge exponentially. If $\lambda \leq 0$ instead the system is not chaotic. An n-dimensional system has n lyapunov exponents, one for each dimension. The Lorentz strange attractor for example has 3 exponent: $\lambda_1 = 0.81$, $\lambda_2 = 0.02$, $\lambda_3 = -14.50$. In order to see if the system is chaotic we have to look at the biggest one, called Maximum Lyapunov Exponent (MLE), in this case λ_1.

Chaos Theory finds applications in a vast variety of sciences like Cryptography where it's used as cryptography primitive, a low-level cryptographic algorithm used to build cryptographic protocols.

Another science that requires the use of Chaos Theory is Meteorology. In fact, knowing that the differential equations governing the convection of air in the atmosphere creates a chaotic system, scientists started using a prediction averaged over an ensemble of initial states in order to make it more reliable. This explains why weather prediction is difficult and reliable only for a few days, indeed, after a longer period of time the initial ensemble becomes more and more detached.

One last interesting field is Economy. Chaos analysis in fact has determined that market prices tend to have a trend. The amount of the trend varies from market to market and from time frame to time frame but the price movements that take place over the period of several minutes will resemble price movements that took place over the period of several years [2].

2 Theoretical Analysis

Chaos can be created using standard electronic components. A circuit, in order to display a chaotic behaviour, needs to respect three simple requirements. It needs to have at least one nonlinear element, at least one locally active resistor and three or more energy storage components.

The Chua's Circuit is the simplest nonlinear dynamical electronic circuit with a strange attractor. It's composed by two capacitors, one inductance (energy storage components), a variable resistance and the Chua's Diode (nonlinear, active resistance) [4].

2.1 Chua's Diode

The Chua's Diode is the nonlinear component of the Chua's Circuit. His I(V) characteristic indeed isn't a straight line rather it has a discontinuous change of the angular coefficient in $\pm E$.

The Chua's Diode is also an active resistor, this means that, apart from $\pm E$ where the slope changes, this component acts like a resistor with negative impedance.

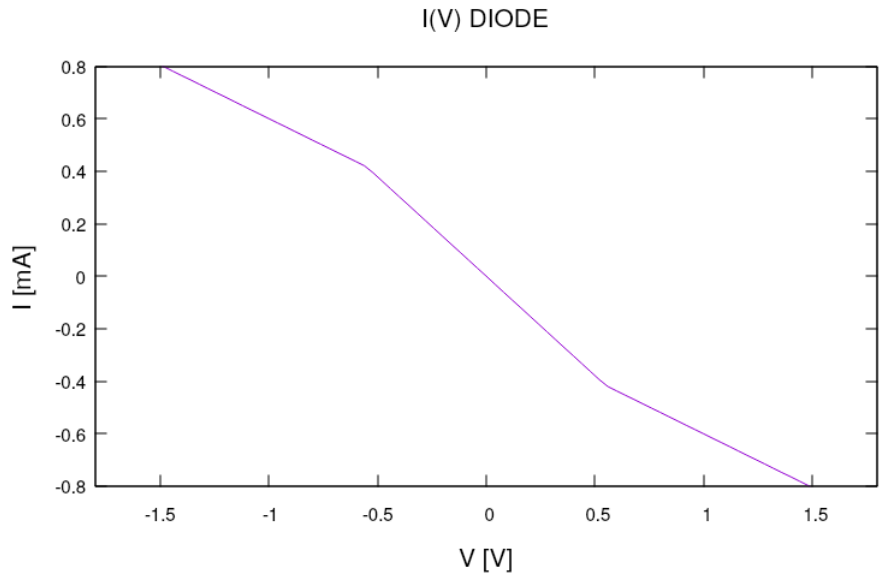

Figure 1: *Desired characteristic of the Chua's diode.*

An electric component with this specific characteristic can be obtained using two NICs (Negative Impedance Converter) 2 and by taking advantage of their saturation behaviour.

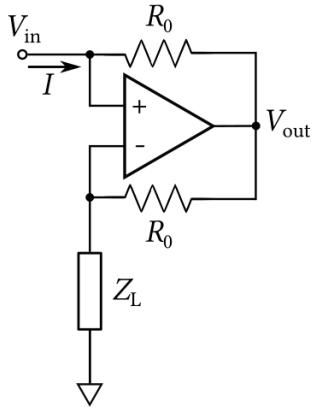

Figure 2: *Negative Impedance Converter (NIC) schematics.*

This circuit is called "NIC" because (in the linear region) the input impedance Z_{in} is equal to Z_L with a changed sign, whatever the load impedance may be. It's possible to derive this relation because when the op-amp is in a stable configuration, as the one shown above, we can assume that $V_+ \simeq V_- \simeq V_{in}$. By noting that V_- is given by the following voltage divider: $V_- = V_{out} \frac{Z_L}{Z_L+R_0}$. We can conclude that the input impedance has the form:

$$Z_{in} = \frac{V_{in}}{I_{in}} \qquad I_{in} = \frac{V_{in} - V_{out}}{R_0} \tag{2.1.1a}$$

$$Z_{in} = \frac{V_{in}R_0}{V_{in}(1-(Z_L+R_0)/Z_L)} = \frac{R_0 Z_L}{Z_L - Z_L - R_0} = -Z_L \tag{2.1.1b}$$

where for the input current we neglected the current flowing into the op amp, considering it as ideal.

Our component unfortunately is not ideal and it cannot output a voltage greater than the voltage supplied to the op-amp. We can calculate the saturation voltage V_{sat} as the maximum input voltage that we can supply to the NIC, such that the output voltage does not exceed the supplied one V_{sup}. This can be done by taking advantage of the voltage divider used previously, $V_{sat} = E = (Z_L\ V_{sup})/(Z_L + R_0)$.

After the saturation threshold the behaviour of the circuit changes, indeed we have that across the top resistor R_0 the voltage difference is $V_{in} - V_{sup}$. The total current that flows through the NIC is then the sum of the max output current that the op-amp can supply $i_0 = E/Z_L$ and the current that flows through the top resistor $(V_{in} - V_{sup})/R_0$. It is now clear that the characteristic of the NIC outside the saturation threshold goes like $1/R_0$.

We can summarize the NIC behaviour like follows:

$$I(V) = \begin{cases} -\frac{1}{Z_L}\ V, & if \quad |V| < E \\ \frac{1}{R_0}\ V \quad \pm i_0, & if \quad |V| > E \end{cases} \tag{2.1.2}$$

One way to implement the Chua's Diode is to use two NICs in parallel. We will call the left NIC the number 1 and the right one the number 2.

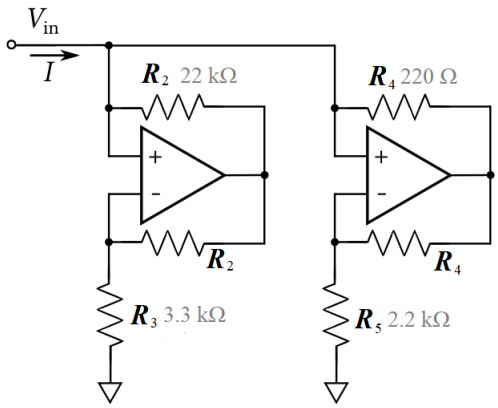

Figure 3: *Chua's Diode schematics.*

It's crucial to notice the differences between R_2 and R_4. This will lead our two op-amps to have very different points of saturation: $E_1 \sim 0.6V$ and $E_2 \sim 4.5V$ (using $V_{sup} \simeq 4.6V$), creating the distinctive change of angular coefficient of the diode. We can finally find the total current that flows into the diode by adding together the currents from the two diodes. We made a C program to simulate the behaviour of the diode and the results are the following:

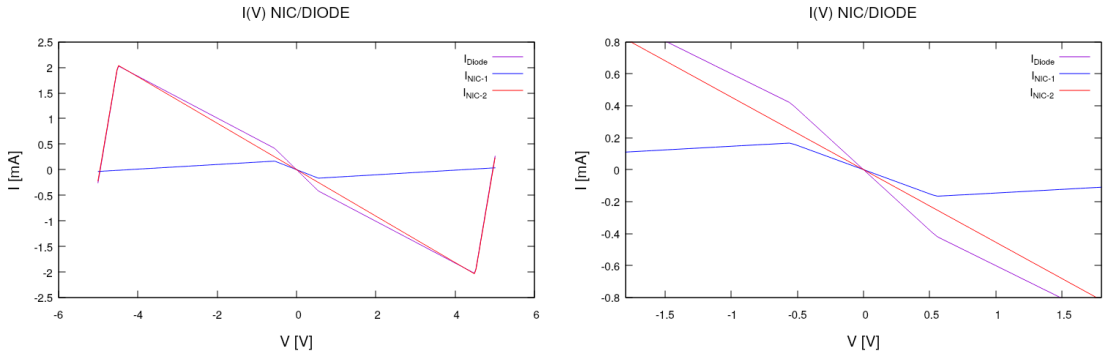

(a) (b)

Figure 4: *Simulated currents of the two NICs and the Chua's Diode*

We can also calculate analytically the semi-ideal behaviour of the Chua's diode [5]:

$$I(V) = \begin{cases} G_c\ V & \pm\left[(G_c - G_b)\ E_2\ +\ (G_b - G_a)\ E_1\right], \quad if \quad |V| > E_2 \\ G_b\ V & \pm\ (G_b - G_a)\ E_1, \quad if \quad E_1 < |V| < E_2 \\ G_a\ V, & \quad if \quad |V| < E_1 \end{cases} \tag{2.1.3a}$$

$$G_a = -\frac{R_3 + R_5}{R_3\ R_5} \qquad G_b = -\frac{R_2 - R_5}{R_2\ R_5} \qquad G_c = \frac{R_4 + R_2}{R_2\ R_4} \sim \frac{1}{R_4} \tag{2.1.3b}$$

2.2 Chua's Circuit

The following schematics 5 represents the Chua's Circuit, as previously said it is composed by one inductor, two capacitors, one variable resistor and the Chua's Diode.

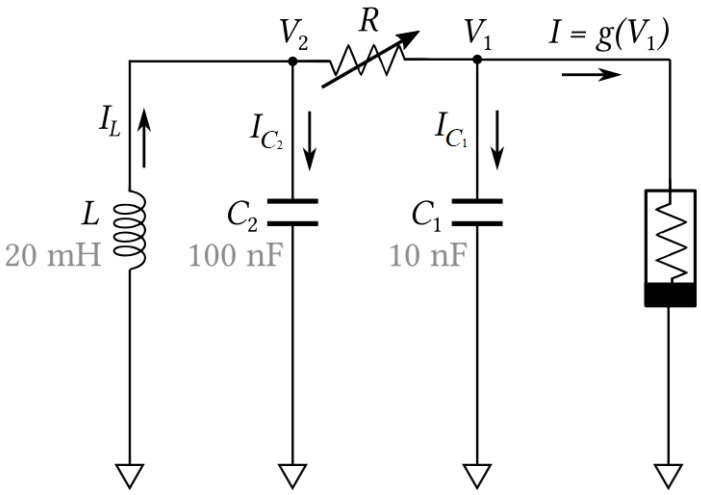

Figure 5: *Chua's Circuit schematics.*

We can extract the three differential equations that rule the circuit using the equations that describe the first three legs of the circuit.

$$\begin{cases} V_2 = -L\dfrac{\mathrm{d}I_L}{\mathrm{d}t} \\ C_2\dfrac{\mathrm{d}V_2}{\mathrm{d}t} = I_{C2} \\ C_1\dfrac{\mathrm{d}V_1}{\mathrm{d}t} = I_{C1} \end{cases} \tag{2.2.1}$$

We can now use the first Kirchhoff law for the V_2 and V_1 knots: $I_L = I_{C2} + (V_2 - V_1)/R$ and $(V_2 - V_1)/R = I_{C1} + g(V)$ where $g(V_1)$ is the I(V) characteristic of the Chua's diode 2.1.3

$$\begin{cases} \dfrac{\mathrm{d}I_L}{\mathrm{d}t} = -\dfrac{1}{L}\, V_2 \\ \dfrac{\mathrm{d}V_2}{\mathrm{d}t} = \dfrac{1}{C_2}\, I_L \;-\; \dfrac{1}{RC_2}\,(V_2 - V_1) \\ \dfrac{\mathrm{d}V_1}{\mathrm{d}t} = \dfrac{1}{RC_1}\,(V_2 - V_1) \;-\; \dfrac{1}{C_1}\, g(V_1) \end{cases} \tag{2.2.2}$$

The fastest way to solve this system of differential equations is using the Runge-Kutta (RK4) [1] numerical method. This algorithm allows us to calculate step by step the solution of a generic differential equation $\frac{\mathrm{d}f(t)}{\mathrm{d}t} = g(f(t), t)$ using a weighted mean of the coefficients K_1 K_2 K_3 K_4.

$$K_1 = g(f_n, t_n) \tag{2.2.3a}$$

$$K_2 = g(f_n + \frac{h}{2}K_1, t_n + \frac{h}{2}) \tag{2.2.3b}$$

$$K_3 = g(f_n + \frac{h}{2}K_2, t_n + \frac{h}{2}) \tag{2.2.3c}$$

$$K_4 = g(f_n + hK_3, t_n + h) \tag{2.2.3d}$$

$$f_{n+1} = f_n + \frac{h}{6}(K_1 + 2K_2 + 2K_3 + K_4) \tag{2.2.3e}$$

In our case we have a system of differential equations. The method is the same used for one equation but instead we need to use a vector $\mathbf{f}(t) = (I_L(t), V_2(t), V_1(t))$ for the solutions and one 3-dimensional vector for each RK coefficient.

We did not use reduced units, instead we used the theoretical value for each component and made the system evolve for 0.03 seconds. We calculated the solutions using 10000 steps and the results, plotted only for a time interval of 8 ms, are the following.

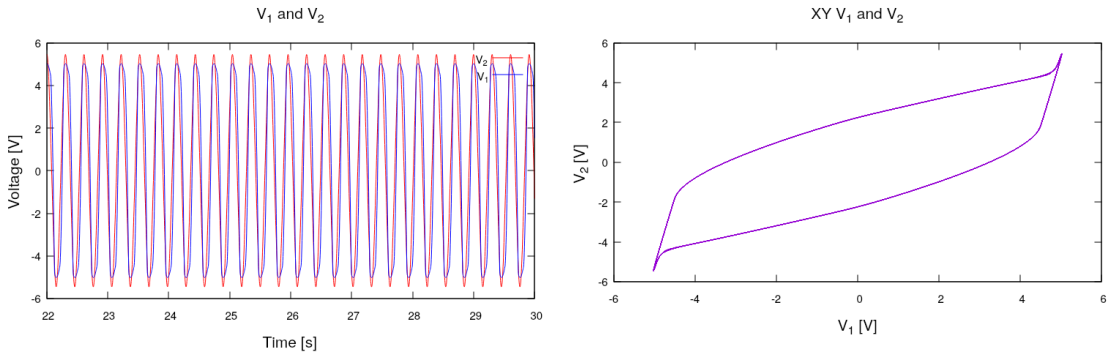

(a) (b)

Figure 6: *Waveforms generated by the Chua's differential equations with* $R = 1.23\ K\Omega$

In the simulation we started with $R = 1.230\ K\Omega$, the solutions of the equations are clearly not chaotic, rather they have a periodic behaviour. We can also notice how both the voltages vary between $\sim \pm 5\ V$ that is where Chua's diode becomes a passive element 4a.

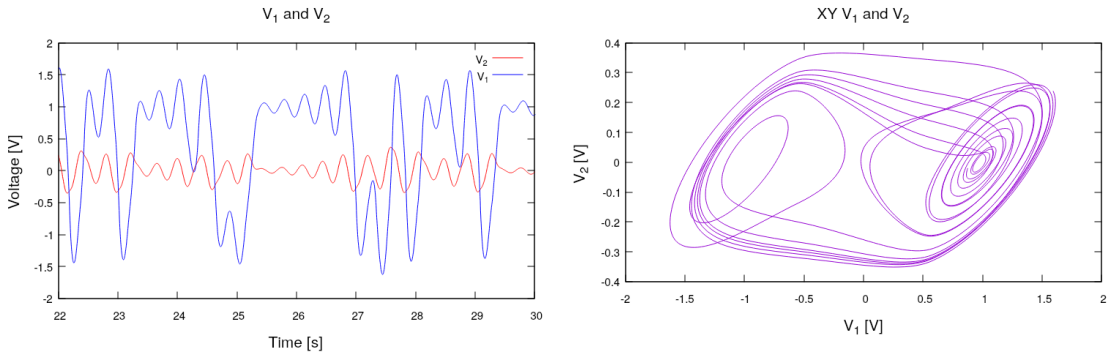

(a) (b)

Figure 7: *Waveforms generated by the Chua's differential equations with* $R = 1.662\ K\Omega$

By setting $R = 1.66\ K\Omega$ instead the waveforms take a stranger shape and an attractor, named "Double Scroll Attractor" shows in phase space. Now the solutions are chaotic.

We also estimated the Lyapunov Exponent by plotting the difference between two different trajectories in function of time $\delta(t) = \sqrt{V_1(t)^2 + V_2(t)^2}$ with a starting difference $\delta_0 = 1\ mV$.

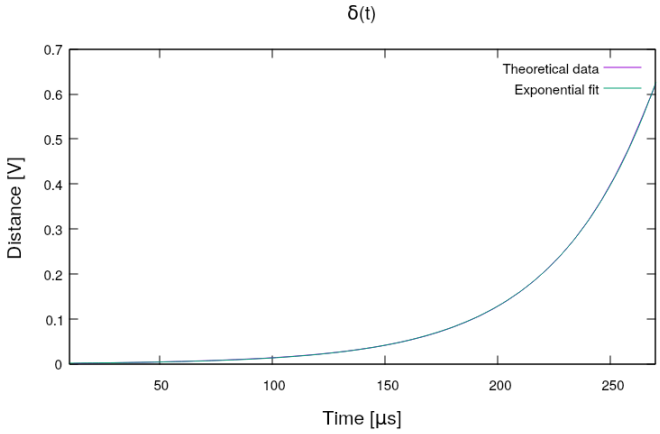

Figure 8: $\delta(t)$ *of two trajectories with initial spacing* $\delta_0 = 1\ mV$.

We used gnuplot to make a fast and simple fit to the function: $f(t) = b + ne^{\lambda t}$ that gave us the following results.

$$b = 0.3 \pm 0.2\ mV \qquad n = 1.40 \pm 0.02\ mV \qquad \lambda = 22.60 \pm 0.04\ ms^{-1} \tag{2.2.4}$$

Being the exponent positive the system is once again confirmed to be chaotic.

This is clearly not the best way to evaluate the Lyapunov exponent but other, more precise, methods require more work. Since is not necessary, for the purpose of this elaborate, to know the exact value of the MLE (Maximum Lyapunov Exponent) we will settle with this easier and faster method.

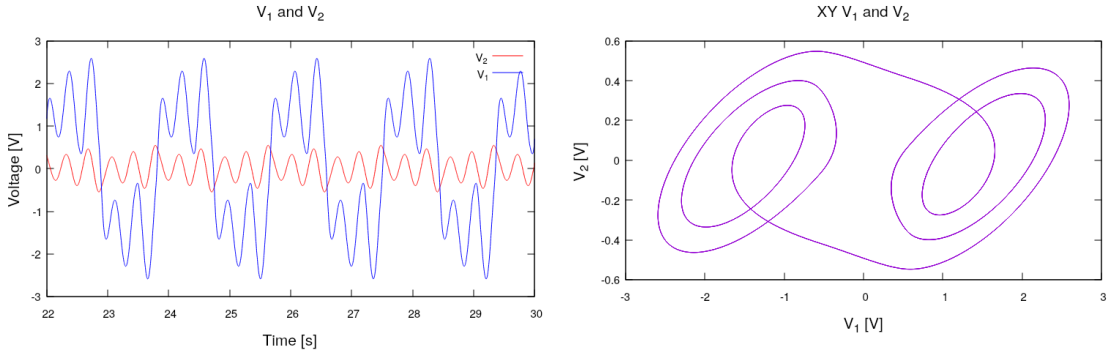

(a) (b)

Figure 9: *Waveforms generated by the Chua's differential equations with* $R = 1.849\ K\Omega$

For some values of the variable resistance the system loses his chaotic behaviour, indeed for $R = 1.849K\Omega$ the solutions are periodic.

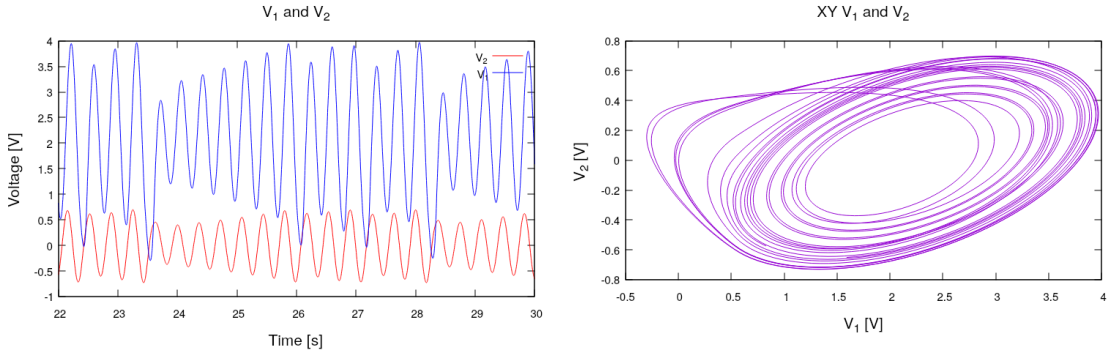

(a) (b)

Figure 10: *Waveforms generated by the Chua's differential equations with* $R = 2.025\ K\Omega$

By increasing the resistance value the system starts to drift into another phase where the chaos is once again the protagonist. The attractor shape on the other hand is changed and now it's named "Single Scroll Attractor".

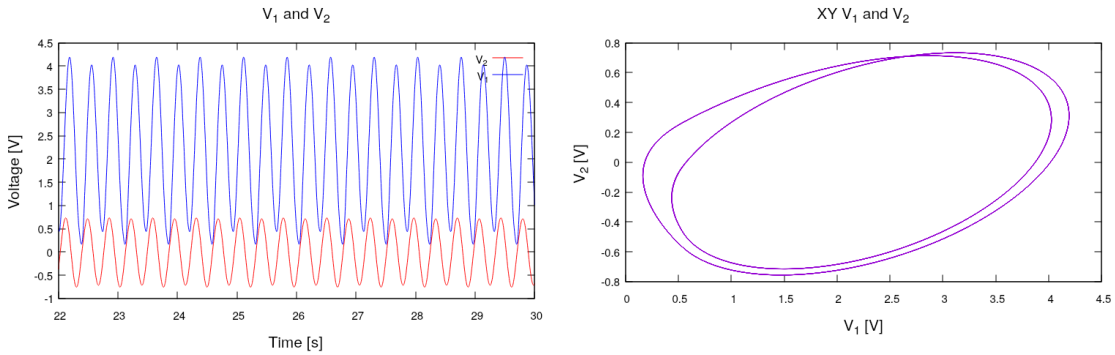

(a) (b)

Figure 11: *Waveforms generated by the Chua's differential equations with* $R = 2.035K\Omega$

The system, as previously said, is not always chaotic indeed after a certain value of R the circuit starts to drift into another periodic solution. For $R = 2.035\ K\Omega$ the shape of the trajectories changes once again. In phase space we can notice the single scroll attractor with a double loop due to the doubling of the amplitude of V_1 and V_2.

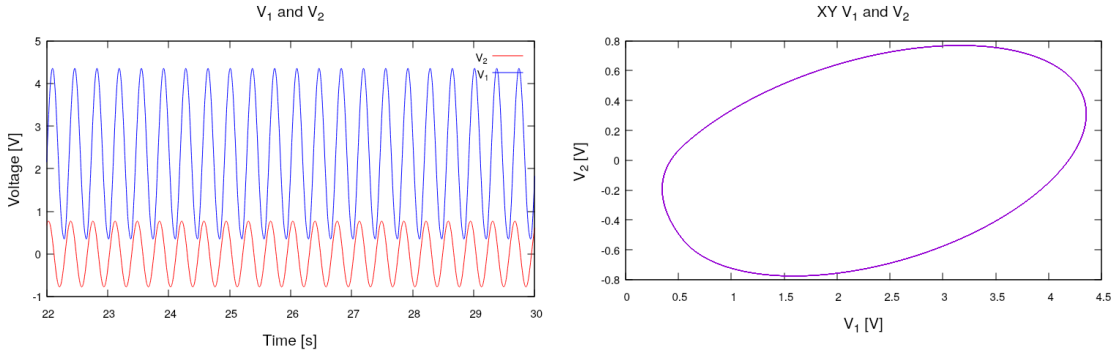

(a) (b)

Figure 12: *Waveforms generated by the Chua's differential equations with* $R = 2.050\ K\Omega$

Finally for $R = 2.050\ K\Omega$ the system reaches his final state, the solutions from now on are always periodic and by increasing the resistance both V_1 and V_2 behave like dumped oscillators decreasing in amplitude and approaching 5 V and 0 V respectively.

We can summarize the behaviour of this circuit in three major phases, "pre-chaos", where the resistance is not high enough to display a chaotic behaviour. In this first phase the solutions of the differential equations are periodic and free to vary from $\sim \pm 5\ V$.

Increasing the value of the resistance then we enter in the chaotic phase. Firstly we can see a double scroll attractor in phase space that will change shape in a single scroll later on. Between the chaos phase there are two small ranges of resistance where the solutions are periodic.

We then reach the "after-chaos" phase. The solutions are still periodic and firstly we can see how they follow the single scroll attractor with an amplitude doubling that will eventually converge to one. For a large enough resistance then the system becomes dumped and the oscillations stop while V_1 and V_2 approach 5 V and 0 V respectively.

3 "RemoteLab"

The "RemoteLab" [7] is a software package created by Alessio Perinelli and Leonardo Ricci with the goal of allowing everybody, equipped with a computer, to experiment with basic electronic circuits.

3.1 Software

There are two softwares that comes with the "RemoteLab" package, a function generator and an oscilloscope. They both exploit the computer's sound card (thanks to the ALSA Library) in order to function while the graphical interface is created using wxWidgets and gnuplot. As it is known, sound can be recreated analogically with an electric signal so, by manipulating this signal we are capable of creating the classic waveforms used in electronics. The standard sound card has two outputs (stereo headphones) and two inputs (stereo microphone) indeed it is capable also to register electric signals as input.

Wavex-generator is the function generator software. It is capable to output the three principal waveforms: sinusoidal, triangular and squared. The output signal frequency range and maximum voltage vary depending from the sound card but is typically from few Hz to $20KHz$ with a maximum amplitude of $\sim 1\ V$.

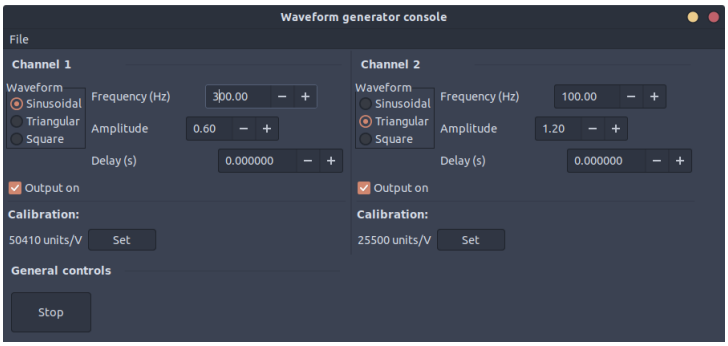

Figure 13: *Wavex-generator interface.*

As we can see from figure 13 the interface is divided in two, one part for each channel. Here we can choose the waveform shape, frequency, amplitude and delay. Once we have chosen all the parameters we can select which channel to turn on. In the "General controls" settings we can then start the function generator.

The working principle of wavex-generator consists in three phases, the first one is the creation of the sound data from the program using the parameters set by the operator. After that, using the ALSA API the data will be written into the sound card that will output it through the 3.5 mm jack. The last step is a check for parameter changes, so when the cycle restarts the output will match the required specs.

The oscilloscope software on the other hand is called Xoscilloscope. Thanks to the sound card this program is capable of acquiring data from the external source and plotting them using gnuplot. For a stereo microphone with dedicated 3.5 mm jack there are two inputs and, as before, the sound card has a limited frequency and amplitude range.

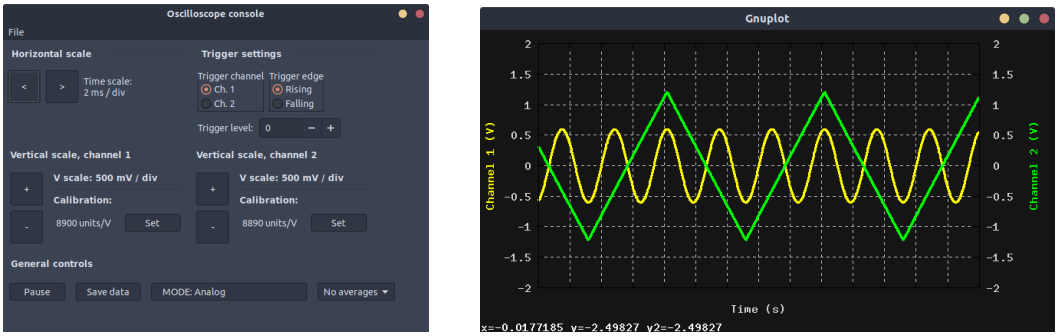

(a) (b)

Figure 14: *Xoscilloscope console and interface*

As we can see from figure 14a the software offers various settings, firstly it allows us to choose which channel is being used as trigger for the oscilloscope. The scales, horizontal and the two verticals ones are chosen separately by the operator. On the bottom part of the interface we can find the buttons for saving the data acquired in that moment, for choosing if the input has been averaged and for changing mode between: analog, x-y, digital and voltmeter.

The working principle of xoscilloscope also consists in three phases. At first the program acquires data from the sound card using the ALSA API, when sufficient data has been stored the waveforms are visualized using gnuplot. The third phase consists in a polling from the console in order to evaluate eventual changes in the settings.

Both softwares need to be calibrated in order to display data in the correct units of measurements. The solution is quite simple, we need to measure a known voltage with the oscilloscope.

The only known voltage in our case is the one supplied to the breadboard, a 5 V DC signal. Measuring this can be tricky because one limitation of using a sound card instead of a real oscilloscope is that the sound card works only in AC coupling because of its design.

Here comes in help the physical interface between software and breadboard. A chopper circuit 16 indeed can be used to transform a DC signal to an AC one; the voltage also needs to be reduceed to 2.5 V to limit the voltage supplied to the sound card and this can be done simply by using a voltage divider. The voltmeter mode on the oscilloscope is specifically made for measuring this type of modified signal.

Once the voltage has been measured, we can easily calculate the units/voltage ratio to calibrate both channels. Once we have a calibrated oscilloscope the calibration of the function generator comes naturally. We need to turn on the function generator, measure the amplitude of our waveforms with the oscilloscope and calculate the units/voltage ratio.

Also the digital mode of the oscilloscope requires the chopper circuit in order to work, this is because we are trying to measure an "on"/"off" signal that is made of respectively 5 V and 0 V.

3.2 Electronic Interface

Connecting the sound card directly to the breadboard could be dangerous for the internal components of the computer. In order to protect them from excessive currents that could flow into the computer we assembled the following buffer circuit that needs to be connected to the oscilloscope probes.

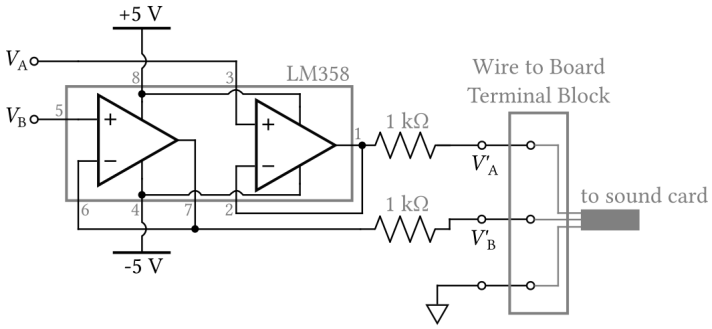

Figure 15: *Input Buffer schematics.*

Other than protecting the sound card, it also has an impedance matching role between the circuitry and our oscilloscope.

As we already said Xoscilloscope is physically limited to work in AC. This is obviously a problem when we are interested in measuring a DC voltage. To get around this inconvenient we need to be able to transform the signal from DC to AC. This is possible by using a chopper circuit as in figure 16.

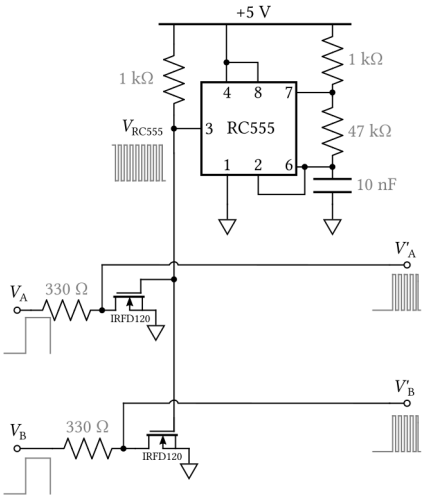

Figure 16: *Chopper schematics for DC signals.*

There is no interface required for the Wavex-generator software but a simple amplifier can be used to achieve bigger amplitudes than the ones generated by the sound card.

4 Experimental Analysis with "RemoteLab"

Apart from the components used to implement the "RemoteLab" interface, the complete list of the components used throughout the experiment is reported below.

Required Components:

- 4 x OP07 op-amps;
- 1 x $R = 10K\Omega$ trimmer,
- 8 x $R_1 = 1K\Omega$ resistors,
- 2 x $R_2 = 22K\Omega$ resistors,
- 1 x $R_3 = 3.3K\Omega$ resistor,
- 2 x $R_4 = 220\Omega$ resistors,
- 1 x $R_5 = 2.2K\Omega$ resistor,
- 1 x $R_{ref} = 2K\Omega$ resistor,
- 1 x $C_1 = 20nF$ Capacitor,
- 1 x $C_2 = 100nF$ Capacitor,
- 1 x $C_3 = 10nF$ Capacitor,

4.1 Chua's Diode

After building the circuit in figure 3, in order to check the correct behaviour of the chua's diode, we need to plot its I(V) characteristic. The current flowing into the diode has been calculated using the voltage difference across a $1K\Omega$ shunt resistance placed right before it, neglecting the current that flows into the oscilloscope. The input voltage has been chosen to be a triangular wave V_t of frequency 100 Hz and amplitude of 0.8 V.

$$i_d = \frac{V_t - V_d}{R_1} \tag{4.1.1}$$

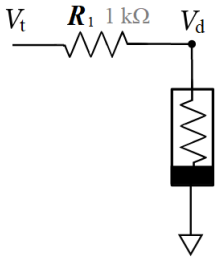

Figure 17: *Schematics for voltage measuring across the Chua's Diode.*

Already by plotting the voltages V_t and V_d we can see both the non linear behaviour of the diode and the active resistance of it.

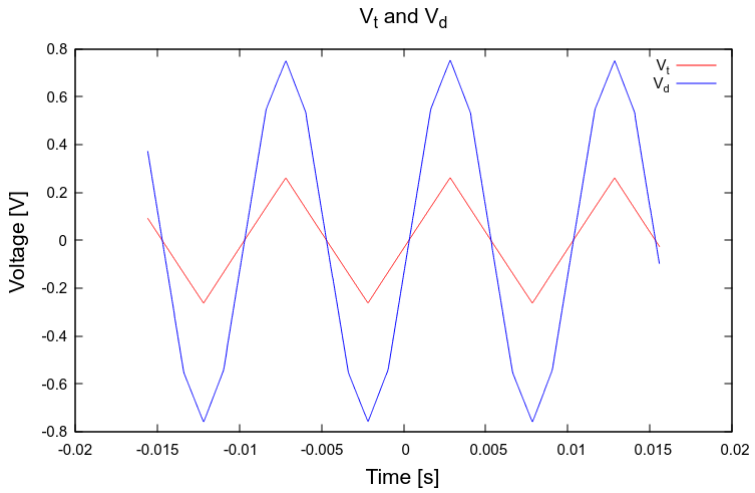

Figure 18: *Voltage across the Chua's Diode in response to a triangular signal of amplitude* 0.2 V.

We implemented a simple C program to extract only one rising slope and then we calculated using 4.1.1 the current flow. Only one slope is enough to verify the correct circuit behaviour since we are not taking specific measurements.

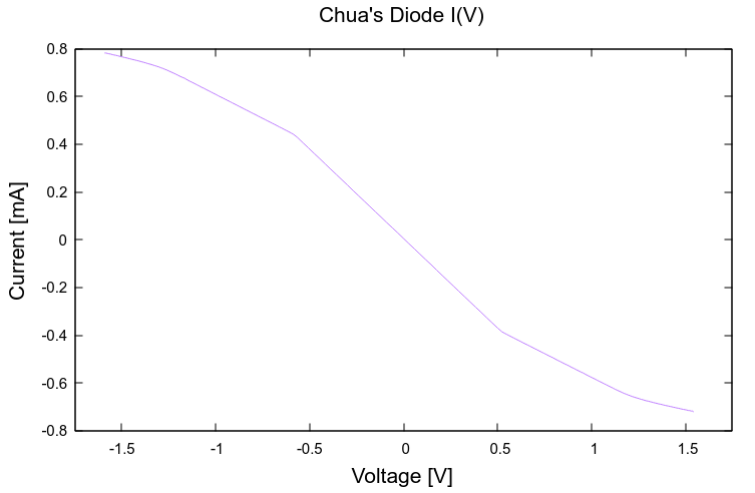

Figure 19: *Experimental I(V) characteristic for the Chua's Diode.*

As we can see from figure 19 and comparing that to figure 1 the diode behaves like expected. The only difference between expected and experimental data is that the empirical ones do not present a precise change of the angular coefficient, rather they show a more continuous and "round" behaviour. This is caused by the fact that our theoretical analysis takes into account an ideal behaviour of our op-amp before and after the saturation while in reality the saturation is not a sudden change of status.

4.2 Chua's Circuit

In order to build the Chua's circuit we need a way to recreate a 20 mH inductor since we did not have one at our disposal. An inductor is an electronic element which his impedance is $Z_I = Ls$. By using two NICs in a "Gyrator" configuration it's possible to reproduce the desired behaviour.

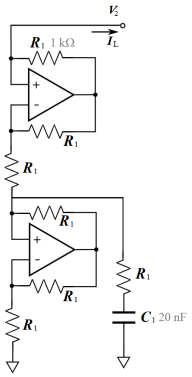

Figure 20: *Gyrator schematics to recreate a* 20 mH *inductor.*

Assuming stability and that we are operating in the linear region of the NICs we can calculate the input impedance of the circuit shown in figure 20:

$$Z_{in} = -[R + (-R)//(R + Z_C)] = \frac{R^2}{Z_C} \tag{4.2.1}$$

given that the capacitor impedance is $Z_C = 1/(sC)$ we can see how the circuit behaves like an inductor $Z_{in} = R^2Cs$ with an inductance of $L = R^2C = (10^3)^2 \cdot 20 \cdot 10^{-9}\ H = 20\ mH$

By adding to the schematics of the Chua's Circuit both the diode and the gyrator we obtain the following circuit.

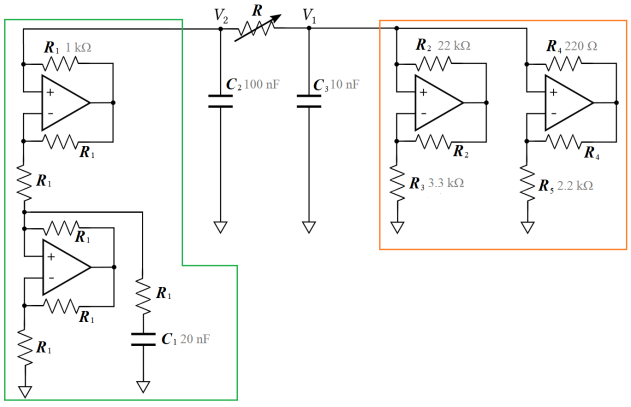

Figure 21: *Complete schematics for the Chua's Circuit. In green we can see the* 20 mH *inductor and in orange the Chua's Diode.*

The circuit behaviour has been studied for 10 values of the trimmer resistance R between $R = 1K\Omega$ and $R = 3K\Omega$. Given that Xoscilloscope is capable of measuring only voltages, the resistance value needs to be calculated using a voltage divider as in figure 22. The voltage reference of $V_{ref} = 5\ V$ given by the breadboard power supply and a reference resistor of $R_{ref} = 2K\Omega$ nominal resistance.

The resistance value of R, indicated as R_X in the schematic, has been calculated using the following formula:

$$R_x = R_{ref}(\frac{V_{ref}}{V_X} - 1) \tag{4.2.2}$$

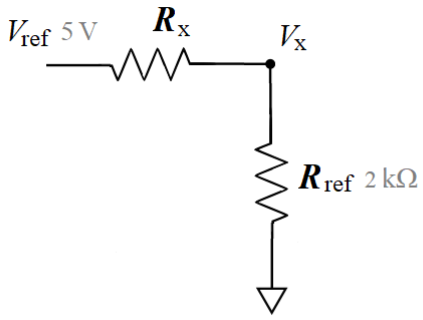

Figure 22: *Schematic for resistance measuring with voltage divider.*

In the following table we can see for each value of V_X measured the corresponding value of resistance R and if a chaos behaviour is displayed by visualizing V_1 and V_2 in the X-Y mode with the "RemoteLab".

Data File	Voltage [V]	Resistance [KΩ]	Chaos
a.dat	3.10	1.23	no
b.dat	2.95	1.39	no
c.dat	2.82	1.55	no
d.dat	2.75	1.63	yes
e.dat	2.67	1.75	yes
f.dat	2.55	1.92	yes
g.dat	2.45	2.08	no
h.dat	2.24	2.46	no
i.dat	2.15	2.65	no
j.dat	1.99	3.02	no

Table 1: *This table gathers all the data acquired for each measurement.*

By looking at all the data acquired during the experiment we can easily recognize the behaviour pattern studied in the theoretical analysis.

For a small enough value of R in fact the waveforms produced by the circuit are periodic 23a. The shape of the trajectory in phase space is very similar to what we expected 6b.

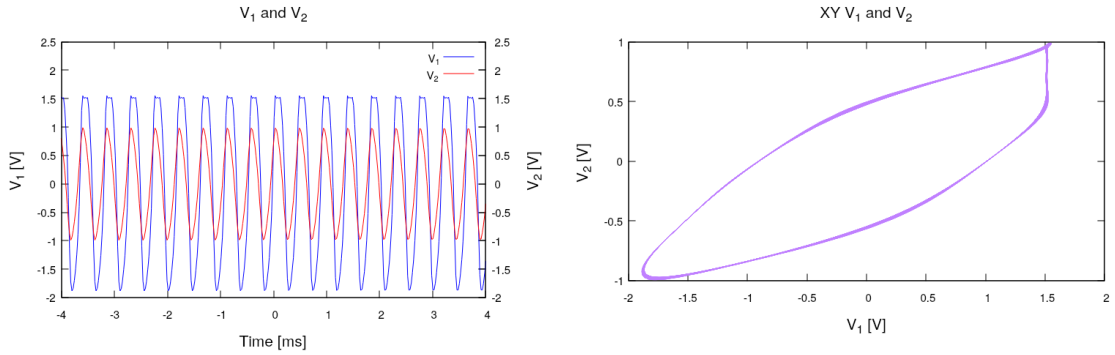

(a) (b)

Figure 23: *Experimental waveforms generated by the Chua's Circuit for the a.dat dataset,* $R = 1.23K\Omega$

Indeed there are some differences between expected and measured waveforms. First of all we can notice how the amplitude of both waveforms are different. The experimental ones in fact have a much smaller amplitude. Also the shape in phase space departs from the theoretical prevision, especially in the bottom left corner, were both V_1 and V_2 are negative.

By increasing the resistance R, the chaotic behaviour of this circuit comes to light.

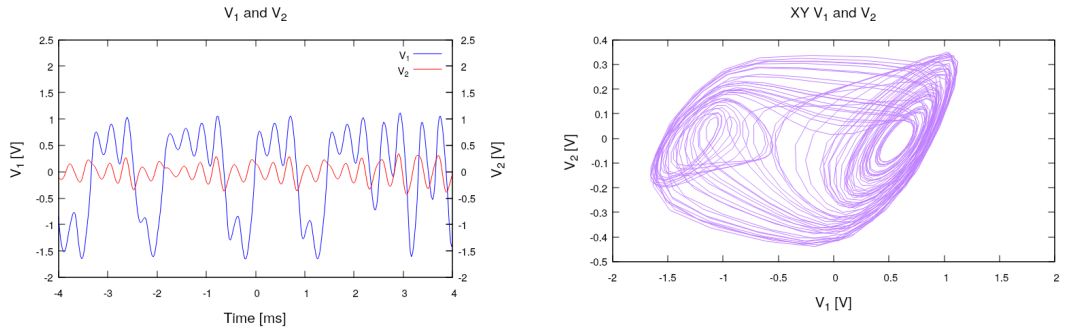

(a) (b)

Figure 24: *Experimental waveforms generated by the Chua's Circuit for the d.dat dataset,* $R = 1.63K\Omega$

The discrepancies in this phase are even smaller then before. The waveforms are still smaller but we can correctly see the attractor in phase space.

After exeeding the $2K\Omega$ threshold our circuit loses its chaotic demeanour.

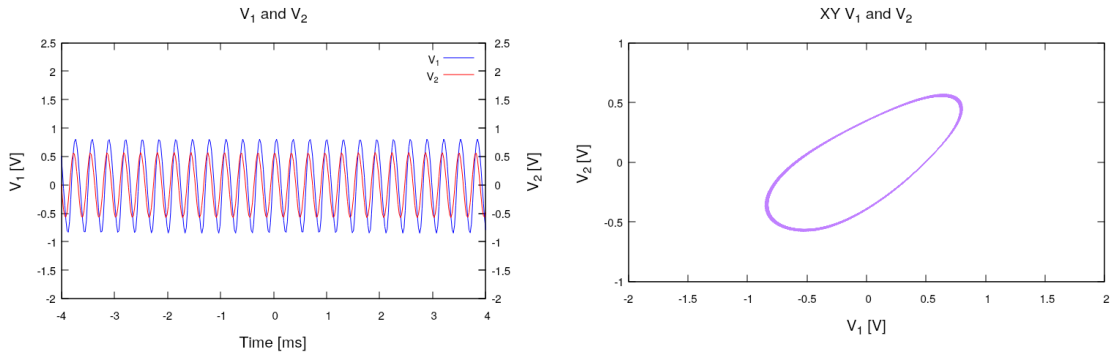

(a) (b)

Figure 25: *Experimental waveforms generated by the Chua's Circuit for the g.dat dataset,* $R = 2.08K\Omega$

In this phase, the expected mean value of V_1 should approach 5 V. The measured one on the other hand does not seem to agree with the expectations. We know that the theoretical behaviour is correct because famous equations such the Chua's ones are already been computed by others [6] with the same results. The experimental waveforms on the other hand has been acquired using the "RemoteLab". This software as said previously utilizes the computer sound card to act as an oscilloscope; being the sound card AC coupled the DC component of our waveforms are neglected. The amplitudes are smaller also in this phase.

After checking the global behavior of the circuit we tried to stabilize the circuit in the two periodic solutions found inside the chaotic behaviour of the circuit, the periodic double scroll 9b and the double period single scroll 11b.

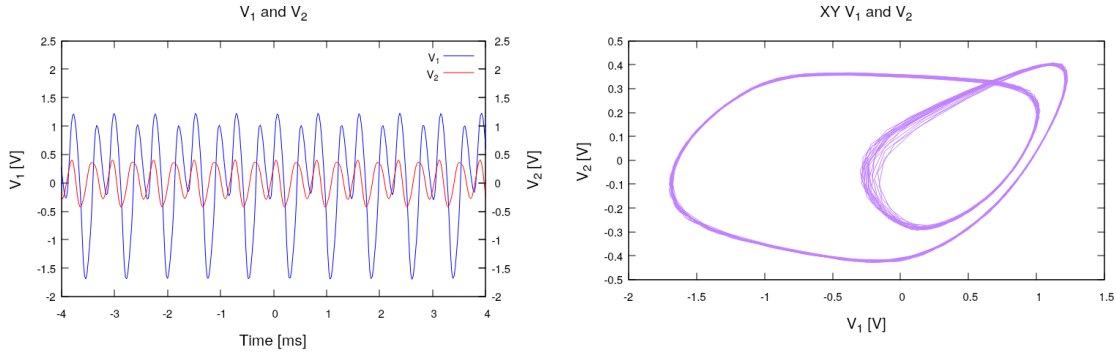

(a) (b)

Figure 26: *Experimental waveforms generated by the Chua's Circuit in the periodic double scroll attractor phase.*

The shape of the measured trajectory 26b resembles the expected one except for the left part of the graph.

The double period single scroll on the other hand is satisfactory even if the voltage spectrum is restricted if compared to the one computed using RK4.

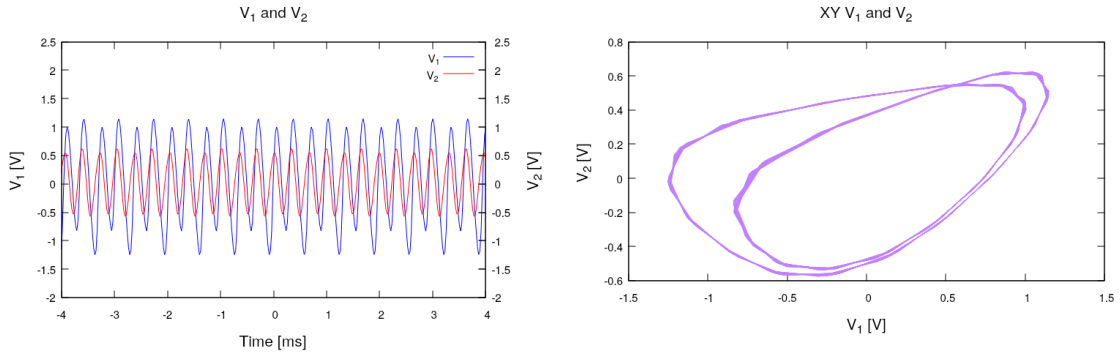

(a) (b)

Figure 27: *Experimental waveforms generated by the Chua's Circuit in the double period periodic phase.*

The system, being chaotic, is very sensitive and both the periodic solutions are unstable and last no more than a few dozens of seconds, for this reason we were not capable of measuring a satisfactory value of the resistance R.

We can finish up by saying that there are three types of discrepancies between the theoretical and experimental waveforms: shape, amplitude and offset.

The offset is the simplest to explain since is only due to the fact that Xoscilloscope is forced to work in AC coupling. In fact every DC component that our theoretical waveform may have is not seen by the oscilloscope.

The differences of the shape in phase space, especially in the negative voltage regions as we can see clearly from 23b-6b and 26b-9b can be attributed to the non ideality of our components.

One last doubt remains, the restricted voltage spectrum. This is caused by the fact that the inductor "L" is recreated using a gyrator. The op-amps inside the gyrator reach the saturation at $E = \frac{R_1}{2R_1} V_{sup} \sim 2.3V$. After this threshold the gyrator behaves differently and changes the differential equations that govern our system. A first, brief study about this effect can be found in the Appendix A.

5 Results and Conclusions

5.1 Chua's Circuit

We successfully verified experimentally the behaviour of the chua circuit for each phase: pre-chaos, chaotic and after-chaos. We also verified the presence of the two periodic solutions while the system was in the chaotic phase. Unfortunately, shape and amplitude of the waveforms captured using the "RemoteLab" are different from the expected ones obtained numerically with RK4.

There is in fact an offset visible especially in the after-chaos phase due to the AC coupling that our instrument has for the way it's constructed.

Other than that, we noticed a different shape of the trajectory in phase space in the pre-chaos phase. In the measured graph we also noticed how the amplitude of the waveforms are smaller and they stop at around 2 V. The problem this time is to be found in how we constructed the circuit. In absence of real inductors in fact we used a gyrator setup that simulates the behaviour of a 20 mH inductor. The gyrator is also made from NICs, and the saturation voltage of those NICs is around 2.3 V since they have the same load and feedback resistance. We are sure that those NICs work both in saturation and non-saturation but in our theoretical model we didn't take that into account.

Adding this correction to our model will decrease the maximum amplitude possible from 5 V to around 2 V as it should. A first attempt was made to take into account the saturation of every NIC inside the circuit but, after a non converging result due to the very approximate model, we understood that a more complex one was necessary.

Being the system chaotic any attempt of measurements is vain. Every time we try to take measurements the system is not the same as it was before. This makes comparing the lyapunov exponent and the critical value of the resistance R impossible. In addition to that, the measurements made with the "RemoteLab" are affected by errors (arising from the calibration) that in this case, where the system is highly sensitive to initial conditions, are non negligible. Despite this the range of resistance is quite similar.

5.2 "RemoteLab" Considerations

The "RemoteLab" platform, being a software that utilizes the sound card as function generator and oscilloscope, cannot give us the same results of instruments that cost thousands of euros.

It has some limitations due to the characteristic of the platform it has been developed on. Our sound card in fact, it has limited range in either frequencies and voltages.

As we said in the previous paragraph it is not the most efficient and precise at measuring voltages. The calibrating mechanism, due to the fact that we are forced to work in AC coupling, takes time and carries experimental errors from the power supply and the nominal value of the resistances used for the voltage divider.

The installation is standard and guided so it shouldn't create problems but someone with some basic linux skills may found it complicated because of the various program dependencies that need to be satisfied by hand.

Nevertheless it is an excellent qualitative instrument to experiment with some electronic circuits. With only a portable computer and a breadboard, that most electronic enthusiasts already have at home, we were able to replace, with some compromises, an actual oscilloscope and function generator and perfectly analyze the behaviour of our circuit. In addition to this is also a great didactic project, were you can learn about electronics and linux just by having fun personalizing it.

6 Appendix

A. First Gyrator Correction

In this section we will analyze a very simple first correction for the Gyrator working in saturation conditions.

When a NIC goes in saturation it behaves like the feedback resistance in series with a current generator. When the top one saturates, so $V_2 > 2.3\ V$, the whole gyrator acts like a resistance. By using this extremely simple correction and using the RK4 method to compute the solutions we obtain the following trajectories in phase space.

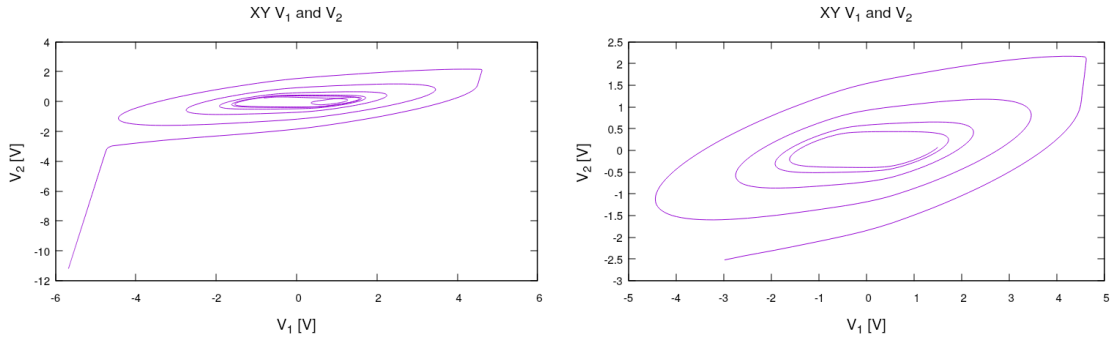

(a) (b)

Figure 28: *Waveforms generated by the Chua's differential equations with the gyrator correction for* $R = 1.650\ K\Omega$.

Both V_1 and V_2 diverge to negative values so this model is clearly not precise enough to take into account the saturation of the gyrator. We should take in consideration the two NICs separately, when only the second one is saturated in fact the impedance of the gyrator becomes:

$$Z_{in} = -[R + (R)//(R + Z_C)] = -\frac{3R^2 + 2RZ_C}{2R + Z_C} \tag{6.0.1}$$

The second NIC goes into saturation when $V_{+2} = V_x$ exceed the $2.3\ V$ threshold. To calculate V_x in function of V_2 we need to use the Millman Theorem and go in the s-domain.

$$\widetilde{V_x} = \frac{\frac{2\widetilde{V_x}}{R_1} + \frac{\widetilde{V_2}}{R_1} + \frac{0}{R_1+Z_C}}{\frac{1}{R_1} + \frac{1}{R_1} + \frac{1}{R_1+Z_C}} = \widetilde{V_2}\left[\frac{s\tau + 1}{s\tau}\right] \tag{6.0.2}$$

One more complex model of the gyrator can be the following

$$\begin{cases} Z_{in} = sL & V_2\ \&\&\ V_x < 2.3\ V \\ Z_{in} = R & V_2 > 2.3\ V \\ Z_{in} = -\frac{3R^2+2RZ_C}{2R+Z_C} & V_2 < 2.3\ V\ \&\ V_x > 2.3\ V \end{cases} \tag{6.0.3}$$

Computing those equations however it's beyond the purpose of this paper.

References

[1] G. Garberoglio. Computational Physics 1, Academic Year 2020/2021.

[2] M. M. H. Hena Rani Biswas and S. K. Bala. Chaos theory and its applications in our real life, 2018.

[3] D. Kartofelev. Nonlinear dynamics: Lecture 9, 2021.

[4] M. P. Kennedy. Three steps to chaos, Part 1: Evolution, 1993.

[5] M. P. Kennedy. Three steps to chaos, Part 2: A Chua's Circuit Primer, 1993.

[6] J. Lavröd. The Anatomy of the Chua circuit, 2014.

[7] A. Perinelli and L. Ricci. Remotelab: Software package for remote laboratory, 2020. URL https://github.com/LeonardoRicci/RemoteLab.

[8] R. L. V. Taylor. Attractors: Nonstrange to Chaotic.